

Optical Engineering

OpticalEngineering.SPIEDigitalLibrary.org

Minimum lifetime of ZERODUR[®] structures based on the breakage stress threshold model: a review

Peter Hartmann

Minimum lifetime of ZERODUR® structures based on the breakage stress threshold model: a review

Peter Hartmann*

SCHOTT AG, Advanced Optics, Mainz, Germany

Abstract. Increasing demand for using the glass ceramic ZERODUR® for optical elements with high mechanical loads called for strength data based on statistical samples larger than 20 specimens. The data now available for a variety of practical surface conditions (ground, lapped, and etched) allow stresses by factors 4 to 10 times higher than before. The larger samples revealed that breakage stresses of ground surfaces follow the three-parameter Weibull distribution. The threshold parameter of this distribution reflects the existence of an upper limit for the microcracks depth within such surfaces. It is equivalent to a minimum strength below which breakage probability is zero. Its use in the well-established crack growth theory allows calculating minimum lifetimes including fatigue using the stress corrosion constant for the prevailing environmental humidity. Long-term loading tests have confirmed the validity of the model. For fully etched surfaces, the Weibull statistics fails because in such cases failure mechanism is not unique anymore. Nevertheless, ZERODUR® with fully etched surfaces that are free from other damages still exhibit minimum breakage stress above 100-MPa tensile stress. The successful satellite mission LISA Pathfinder has confirmed the possibility to apply ZERODUR® for utmost precision experiments together with high mechanical loads. © The Authors. Published by SPIE under a Creative Commons Attribution 4.0 Unported License. Distribution or reproduction of this work in whole or in part requires full attribution of the original publication, including its DOI. [DOI: 10.1117/1.OE.58.2.020902]

Keywords: ZERODUR® strength; breakage stress; ground surface; etched surface; Weibull distribution; LISA Pathfinder.

Paper 181512V received Oct. 24, 2018; accepted for publication Jan. 14, 2019; published online Feb. 9, 2019.

1 Introduction

The key property of the glass ceramic ZERODUR® is its extremely low-thermal expansion.¹ Equally and sometimes even more important is the very high homogeneity of this property throughout the total volume of very large items.² Both together are the essential criteria deciding on the application of the material. However, additional requirements such as withstanding high mechanical loads can exclude ZERODUR® despite its excellent performance in terms of thermal behavior.

In most applications, there are no special requirements on the resistance of optical materials to mechanical loads. Supports and frames serve to hold just the optical element's own weight. In such conditions, the tensile stress loads on the surfaces are fairly low. If they are below 10 MPa (mega-Pascals), there is no need for any special analysis. This is a safe value for tensile stress loads on ZERODUR® surfaces. However, it is also a quite low value. An increasing number of applications rely on higher mechanical strength thus triggering the review of the available data and information about the breakage strength of ZERODUR®. Furthermore, the conditions to improve the reliability of strength and lifetime calculations were thoroughly investigated. The specific cause for starting extended investigations in 2007 was the satellite project LISA Pathfinder. This space mission combined the requirement of utmost length precision with high mechanical strength.³ ZERODUR® is used as the optical bench for laser interferometry and as a clamping frame keeping all elements of the experimental setup together, the optical bench, and two inertial mass containers. The strength data base of

ZERODUR® was not sufficient for a reliable assessment of its suitability to withstand the short time but high 20g vibration load of a rocket launch. For this reason, SCHOTT started a measurement campaign together with EADS Astrium with the aim of obtaining larger samples allowing future prognosis with much better confidence.⁴ SCHOTT is a Germany-based company manufacturing optical glass and the extremely low-thermal expansion glass ceramic ZERODUR®. EADS Astrium now called Airbus Space is the space division of Airbus, a European Aerospace company.

The results of the measurements exceeded the original aims of the campaign by far. Enabling a considerable improvement of the lifetime calculation model for ZERODUR® structures, it is now possible to predict their endurance with long-time loads lasting over many years. One example for such loads is bonded fixtures of mirror segments to support frames, which are planned for the European Extremely Large Telescope (ELT).⁵ Glued bonds exert forces to the glass-ceramic due to glue shrinkage stress. Additional forces arise from the weight changing with different observation angles and from the inline segment shape optimization. All fixtures shall hold reliably during the total telescope life time of many years.

The key factor deciding about the breakage strength of a glass or glass-ceramic item is its surface condition. Glass items with perfectly smooth surfaces withstand very high stress, much higher than 1 GPa. As soon as there are microcracks in the surface strength drops down by two to three orders of magnitude. Such microcracks grow if the surface tensile stress is large enough to rip the atomic bonds at the crack tips apart.⁶ At low stress, this growth may be too small to result in any macroscopic changes or there may be even no growth at all. At high stress, crack growth speeds up until it

*Address all correspondence to Peter Hartmann, E-mail: peterhartmann17@gmail.com

reaches a very high value ending up in fast macroscopic breakage of the glass object, see Sec. 4.

In addition to stress, the initial depth of the microcracks is another factor that influences their growth rate. In a stress loaded area, there may be some few microcracks for example in polished surfaces while in ground surfaces there may be even many thousands. Their depths are statistically distributed. For the breakage resistance, the deepest microcrack is the relevant one. In each area under consideration, there is one deepest microcrack. The depth distribution of these deepest microcracks follows the Weibull extreme value statistical distribution. It is widely used in glass and glass-ceramic strength analysis for fitting breakage stress samples.^{7,8}

Before 2007, only small samples with sizes up to 20 specimens were available. Thus the main task was to increase the sample size up to 150 specimens. However, this did not only improve statistics, but also revealed a different statistical distribution much more adequately representing the data than the one used before.⁹ Although the two-parameter Weibull distribution fitted the small samples sufficiently well, the large samples revealed significant deviations, most importantly at lower stresses. The new data drop much faster than predicted by the two-parameter Weibull distribution. Finally, even a stress limit value is approached. Applying the three-parameter Weibull distribution, the data are much better represented. Its third parameter is a stress offset value or breakage stress threshold value. The existence of this threshold fits much better to the existence of an overall maximum microcrack depth, which is expected for surfaces prepared with well-defined machining processes. This is an upper limit for the microcrack depths of all local deepest cracks. Such limit has been observed in a variety of investigations using different methods, see Sec. 6.

Since 2007, a considerable number of large breakage stress samples have been obtained.¹⁰ Based on these results, the three-parameter Weibull distribution is now proven to be valid for ground surfaces. The discovered breakage stress threshold is highly valuable. It shows that there is a stress range where breakage probability is zero. This is a tremendous gain in reliability of strength calculations.

Common measurement methods allow for determination of the threshold breakage stress for loads usually lasting as short as 1 min or less. Obviously, this is not sufficient for calculating the admissible stress for long-lifetime applications. There might be a strength degradation with time in glass-ceramics and glass materials. This fatigue effect occurs only when surface tensile stress and a fatigue agent such as water is present.⁶ The theory of stress corrosion allows taking fatigue into account. This method of calculating the growth of subsurface microcracks is well established. In effect, it leads to shifting the short-term threshold stress to lower values with time. It allows to predict minimum lifetimes for given constant stress loads or calculating the maximum permissible stress for a required minimum lifetime.¹¹ A verification experiment with long-term constant loads supports the validity of the deterministic life time prediction method, see Sec. 8.

The experimental results allow stress loads 4 to 10 times higher than before depending on the surface preparation and conservation. This opens up a wide field for new applications. The application case for the project, which has started

the strength investigations, LISA Pathfinder began on December 3, 2015 when it was launched to its orbit. The project has turned out to be extremely successful. Its launch survival was a necessary precondition.

2 Bending Strength Depends on Surface Conditions

2.1 Strength Reduction as a Result of Microcracks

Glass and glass ceramics are brittle materials. The strength of their atomic bonds indicates them as very strong materials. However, in common practical applications, their strength lies several orders of magnitude lower than calculated from their atomic bond energies. The reason is their high sensitivity against surface microcracks introduced by environmental influences.¹² They are the starting point of crack growth, when surface tensile stress exceeds a threshold value. All stress energy will be converted into crack progression. There are no other energy consuming mechanisms such as plastic deformation due to strain as existing in metals.

Strength of brittle cast materials is all about subsurface microcracks. The main task thus is to characterize surface conditions with their associated microcracks and their consequences with respect to breakage behavior. For long-lasting loads, slow subcritical crack growth under tensile stress—stress corrosion—must be taken into account as fatigue effect.

Most commonly used everyday glass items have fire polished surfaces. These surfaces emerge during casting and hot forming of glass. During the use, they wear by scratching with harder materials thus acquiring microcracks or larger cracks. If a mechanically or thermally induced surface tensile stress acts on them they might eventually break.

The surfaces of optical elements such as lenses, prisms, and mirrors are generated by grinding, lapping, and polishing depending on their functional requirements. In the case of mirrors, there are at least two surface qualities present. The mirror surface is polished, while the rear side and the edges are usually ground.

The mirror surface preparation is a multistep process starting with a grinding process and ending with polishing. According to good optical workshop practice, which means processing in several steps with ever smaller grains being used, the final surface is free from subsurface microcracks. As a consequence, the optically polished face is the mechanically strong part of the mirror. The ground lateral and back sides exhibit microcracks making them the weaker parts of the mirror. So they are relevant for the mirror's lifetime.

2.2 Microcrack Depth Determination

The microcracks must not be confused with surface roughness. They start from some points at the rough surface and extend up to 4 or 5 times deeper into the material than the roughness peak-to-valley value, see Fig. 1. The very tips of the microcracks cannot be seen. Their cleavages approach atomic dimensions, which cannot be resolved with common optical observation methods. For this reason, neither the starting point in the rough surface nor the tip of a microcrack can be detected with high accuracy. Due to the need for cross sections in order to characterize surface microcracks on a three-dimensional sample, it is absolutely impossible to identify the deepest microcrack let alone to determine its depth

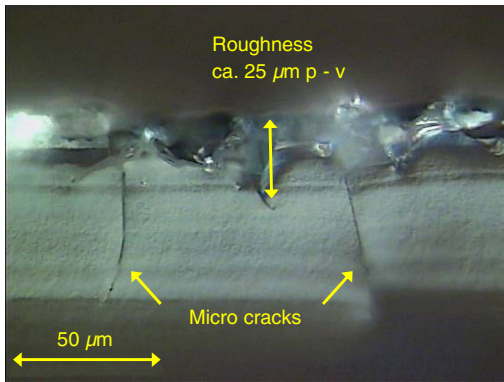


Fig. 1 Optical micrograph of the cross section of a D151 ground ZERODUR® surface. Two microcracks extend into the bulk material with very narrow cleavage not accessible to a roughness measurement stylus tip. Surface roughness is about 25 μm p-v. The microcracks are deeper than 50 μm . The distance is about 70 μm .

with the precision necessary for reliable lifetime calculations based on fracture mechanics.^{13,14} The precision requirement is high since the crack depth finds itself in the microcrack growth equation [see Eq. (5) in Sec. 4] in the basis combined with a high exponent. Small variations in the initial crack depth value lead to huge changes in crack growth rate by orders of magnitude preventing any lifetime prediction with reasonable accuracy.¹³

2.3 Ground Surface Specimens as Elements of Experiments

In order to circumvent the microcrack depth determination problem, breakage statistics has been investigated intensely. The use of specimens with surfaces ground like optical elements' faces allows an easy transfer of the results to practical cases. Grinding is done with rotating tools moving along predefined paths in order to achieve the desired face shape. The tools are wheels or cylinders with the working edge consisting of diamond grains bonded in a carrier material. They are specified by their diamond grain size distribution, which results from sieving grains with meshes of standard widths. For example considering a D151 tool, the D stands for diamond and the code 151 means a maximum grain size of 150 μm . Additionally, the one at the end indicates the narrow size distribution 125 to 150 μm .¹⁵ Such tools typically serve for final shaping of back and lateral faces. Finer grains commonly used for smoother surfaces with smaller microcracks are D64 and D46 with 63- or 45- μm maximum grain size, respectively.

Grinding introduces surface cracks by its nature. Taking off glass layers requires scratching cracking and removing glass chips by moving the diamond grains with high speed and with pressure across the glass surface. One essential question is if microcracks generated this way can be arbitrarily deep with lower occurrence probability for larger cracks. Or if there is a general limit, which is related to the diamond grain size and the force pressing them into the glass. The answer decides on the statistical distribution which is valid for the breakage stresses. If a maximum microcrack depth exists this should be reflected by a minimum breakage stress, the stress threshold of the three-parameter Weibull distribution. All observations with SCHOTT

ground ZERODUR® surfaces confirm the existence of a maximum microcrack depth. For D151, it is about 110 μm .

Another important question is, is it possible to increase strength by a considerable amount? The main practical possibilities are reducing microcrack depth using finer grains and removing microcracks by acid etching or by polishing. This work concentrates on using finer grains and acid etching, because they are easier and cheaper to apply than polishing.

3 Breakage Measurement and Results for Ground ZERODUR®

3.1 Test Setup, Specimens Preparation, and Measurement

The target is to find the dependence of breakage failure probability on surface tensile stress for a given surface condition. The common measurement method is breaking a sample of specimens in a double ring test setup according to the European standard EN 1288-5,¹⁶ see Figs. 2 and 3(c). A rectangular tile or disk lies on a support ring with the surface to be tested downward. Applying a force on the load ring from above leads to tensile bending stress on the lower surface. The double ring setup with the diameter ratio of 5:1 has the advantage that within the area opposite to the load ring stress is constant and isotropic. The stress falls off sharply toward the support ring thus concentrating breakage origins within the load ring area. The stress at the lower surface opposite to the load ring area can be calculated from the material's Poisson's number, the thickness of the specimen, the setup geometry, and the force using a simple equation, which is given in the European standard EN 1288-1.¹⁷ Stress will be raised linearly usually with 2 MPa/s until the specimen breaks. The breakage stress will be recorded. Specimens will be accepted for evaluation only if their breakage origin lies within or at the edge of the load ring, because in this area stress is unambiguous and calculable.

The tiles were made starting from a 1.5-m diameter plate of ZERODUR® with about 10-mm thickness. The side to be tested was ground with a D151 tool taking off more than 1 mm. This served to remove the subsurface microcracks introduced by the D213 diamond grain pellets of the wire saw, which was used for cutting the plate from a thick disk. If D151 tiles were the target, grinding continued to the final thickness of 6 mm. For D64 fine ground tiles, final thickness removal was 0.5 mm at minimum. For finest ground surfaces such as D25, the sequence contained a 0.5-mm D64 intermediate step for the removal of the D151 microcracks. The final grinding step reduced thickness by at least 0.2 mm to remove the D64 microcracks. These precautions served to assure that the tiles' surfaces to be tested were typical for the tool and process to be investigated and that no microcracks from preceding processes with

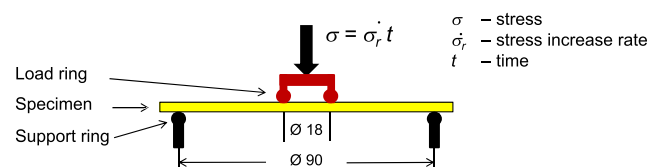


Fig. 2 Ring-on-ring test setup for breakage stress measurement principle.

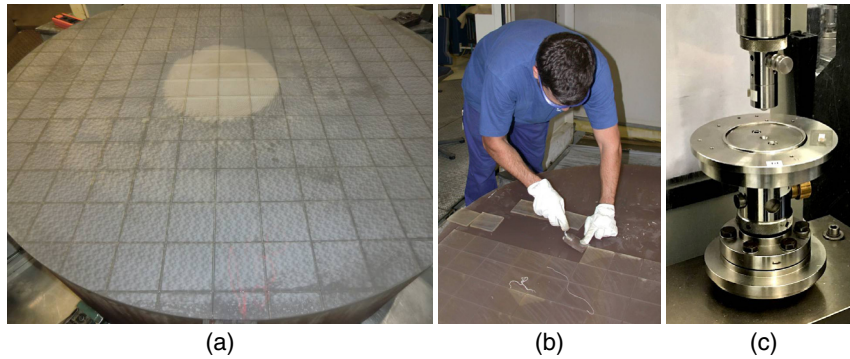


Fig. 3 (a) Ground ZERODUR® disk with cut ground tile pattern, (b) isolating 100 mm × 100 mm × 6 mm tiles for breakage stress measurement, and (c) laboratory ring-on-ring setup.

larger diamond grains remained. The plate’s rear side was ground taking off more than 0.5 mm with a D151 tool. One obtains isolated tiles by grinding grooves in a rectangular pattern into the plate with a thin wheel down to <1-mm thickness and by breaking the tiles apart see Fig. 3(a) and (b). This renders a large set of quadratic tiles ready for the breakage tests. The high number of specimens (100 to 170) per sample achieved in this way provides statistical distributions with much better significance than before. For the investigation of etched surfaces, the tiles underwent an etching process after grinding removing a layer of thickness close to or exceeding the maximum microcrack depth. The acid used was a mixture according to the Schott standard recipe.¹⁸ Breakage stress for etched tiles can exceed that of ground tiles by a factor higher than 10 as was shown in this investigation. A considerable share of tiles breaks outside the load ring thus reducing the number of valid specimens.

3.2 Data Evaluation

The common way of sample evaluation is to plot the recorded breakage stress data $\sigma_B(i)$ obtained with the ring-on-ring test setup in a cumulative Weibull diagram.

Due to its special axis scales, it needs some preparation of the data. The first step is sorting the data according to their size and assigning their rank index i . Next follows the calculation of the relative nominal failure probability for each breakage value $\sigma_B(i)$ according to the Bernard and Bosi–Levenbach approximation for median ranks,¹⁹ see Eq. (1), with N being the total sample size. Inserting the failure probability values $F[\sigma_B(i)]$ into Eq. (2), which is derived from the Weibull distribution function [Eq. (3)], leads to the ordinate values y_i for the diagram

$$F[\sigma_B(i)] = \frac{i - 0.3}{N + 0.4}, \tag{1}$$

$$y_i = \ln \left(\ln \left\{ \frac{1}{1 - F[\sigma_B(i)]} \right\} \right). \tag{2}$$

To obtain the diagram, the ordinate values y_i for the failure probability values $F[\sigma_B(i)]$ are plotted against the abscissa values $x_i = \sigma_B(i)$ on a logarithmic scale. Rescaling the y axis to the failure probability in percent allows easier reading as shown in Fig. 4. The advantage

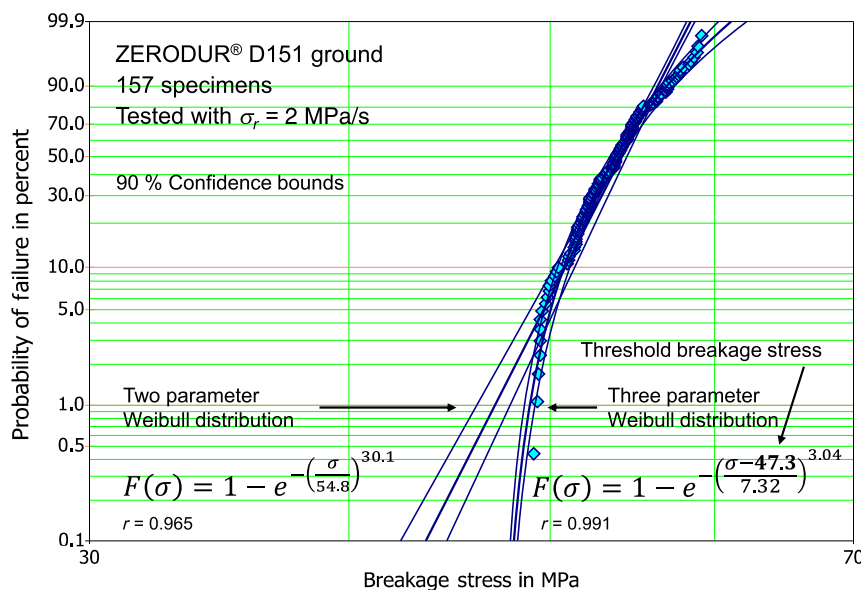


Fig. 4 Weibull plot of a ZERODUR® D151 sample with two- and three-parameter cumulated Weibull distributions fitted and 90% confidence bounds. The sample approaches the threshold stress at 47.3 MPa.

of this diagram is that a sample of specimens that exactly follows a three-parameter Weibull distribution shows the curvature of the distribution toward a certain threshold stress very clearly. A different sample following a two-parameter Weibull distribution would lie on a straight line. A least-squares fit program yields the three parameters of the Weibull distribution the scale parameter η , the shape parameter β , and most important for breakage stress distributions the threshold stress σ_T . Figure 4 shows the Weibull diagram for ZERODUR® D151 ground surface data together with the best-fit three-parameter Weibull curve and the best fit two-parameter Weibull straight line as well as the two 90% confidence bounds for each case.

The Weibull distribution is an extreme value statistical distribution, which is based on the weakest link model. The three-parameter version is given by Eq. (3). The two-parameter version is derived if $\sigma_T = 0$ ²⁰

$$F(\sigma) = 1 - e^{-\left(\frac{\sigma - \sigma_T}{\eta}\right)^\beta}, \quad (3)$$

σ_T is the location parameter—threshold stress, η is the scale parameter, and β is the shape parameter.

Best fits require that the weakest link precondition is given and that there is only one failure mechanism present in the data sample. Data samples should be monitored to ensure that they were prepared homogeneously. The checking method used is evaluating patterns of the color-coded breakage stress within a tiles location map.²¹ For etched surfaces, the unique failure mechanism condition is not valid anymore (see Sec. 6). Here the Weibull fit usually fails by yielding a negative threshold stress value.

Additionally, breakages starting from isolated deeper scratches of different origins than the grinding process might obscure the underlying Weibull distribution. Such scratches can come from diamonds breaking off their bonds and moving across the surface or from violent tool motion under adverse grinding conditions. It is important to scrutinize outliers and shape deviations before including them in or excluding them from the data sample.²¹

Each data point of the sample in Fig. 4 represents a breakage starting from the deepest of about 50,000 microcracks. Such huge number is present in the 254-mm² loaded area of a single tile in the test setup of Fig. 2. This number is roughly estimated from an average distance of 70 μm between two deep microcracks see Figs. 1 and 8. The data displayed in Fig. 4 are based on a total loaded area of about 400 cm². The number of about 8 million microcracks underpins the statistical relevance of the results.

3.3 Three-Parameter Versus Two-Parameter Weibull Distribution

The traditionally used two-parameter Weibull distribution leads to several misconceptions all pointing into the direction of predicting lower strength than actually exists.²¹

At first, it predicts finite failure probability even for very low-stress values. Data samples do not support this. There is no physical reason for low-stress failure. The fact that in any area under consideration a microcrack with maximum depth exists contradicts such predictions.

The two-parameter Weibull distribution-based predictions of failure probability for low stress are contradictory. For surface conditions known to be stronger than coarse ground

surfaces such as fine ground, polished, or etched surfaces failure probability at low stress should be lower, too, as experimental observations confirm. Two-parameter Weibull distribution-based analyses predict higher failure probability, instead. The reason is that the higher lying breakage stress distributions of stronger surfaces are broader as numerous investigations have shown. Fitting the two-parameter Weibull distribution to such samples leads to straight lines with shallower slopes than those for coarse ground surfaces. Such lines extrapolated to low-stress values result in higher failure probability than those obtained from weaker samples with steeper slopes. Considering the microcrack depth distribution of an etched surface the extrapolated two-parameter Weibull distribution down to low stress implies low failure probability but different from zero. This means that etching of a ground surface would not just remove the microcracks from grinding. It could also introduce cracks deeper than those of the preceding ground surface. There is no physical process associated with etching or polishing, which could explain this. Therefore, predictions of failure probability at low-stress values based on extrapolated two-parameter Weibull distributions are wrong.

Moreover, the two-parameter Weibull distribution predicts an area dependence of strength. In strength analyses, the area factor leads to a further reduction of the allowable tensile stress. The area dependence can be illustrated by Fig. 4 considering the data sample shown. One dot corresponds to a tested area of 254 mm². Each dot adds a tested area of the same size. If the low-stress data followed the two-parameter Weibull distribution more and more data points would appear on the straight line toward low failure probabilities. The experimental data, however, show a different behavior of the breakage stress rapidly approaching a threshold stress. Below this threshold stress there is no area dependence anymore and there is no need for an area factor.

For homogeneously ground surfaces, the adequate statistical representation is the three-parameter Weibull distribution as it is justified from the existence of maximum microcrack depths and supported by experimental data. This distribution has the invaluable advantage of predicting failure probability equal to zero for stress values below the threshold stress σ_T . The reaction on stress loads below σ_T is purely deterministic thus strengthening confidence in load endurance considerably.

3.4 Results for Ground ZERODUR®

Figure 5 shows measurement results for ZERODUR® depicted in a Weibull diagram. The samples represent surfaces prepared by grinding with diamonds grains of five different maximum sizes (D151, D64, D46, D35, and D25) and by lapping with silicon carbide of two different maximum grain sizes (SiC320 and SiC600). The maximum grain sizes of D151, D64, and D46 follow the rule of the standard ISO 6106¹⁵ with 150, 63, and 45 μm . D35 and D25 are microgrit grain specifications, which are not standardized but supplier dependent. Their maximum grain sizes lie below 40 μm . The maximum sizes of the SiC loose lapping grains are 49 μm for SiC320 and 19 μm for SiC C600.

All samples fit to three-parameter Weibull distributions very well. The table in Fig. 5 lists the Weibull distribution parameters, the minimum and maximum breakage stress

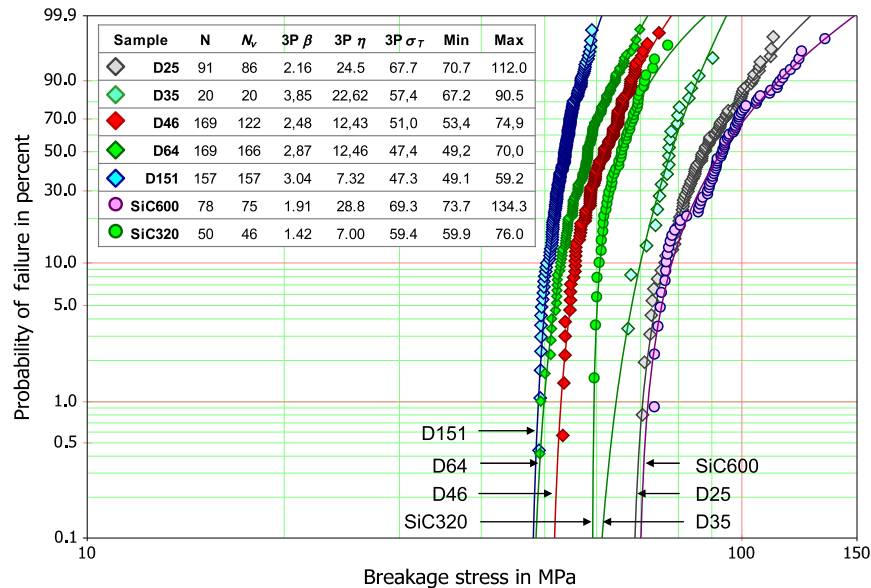


Fig. 5 Weibull plot for samples of ground (D) and lapped (SiC) ZERODUR®. D151, D35, and D25 ground with a flat rotating tool, D64 and D46 with a rotating edge tool. The table contains the sample size and the number of valid specimens, the Weibull distribution fit parameters, as well as the maximum and minimum breakage stress values of the samples.

values found, the sample size N and the valid number N_v of specimens broken regularly in the loaded area. The results are valid for short-time loads of about 1-min duration.

The threshold breakage stresses of the D151 and D64 samples are almost the same, which is surprising considering the large difference in the maximum grain sizes. Partly, this can be explained by different grinding kinematics. The D151 sample has been prepared with a flat rotating tool, which tends to generate less deep microcracks than the rotating edge tool, which was used for the D64 and D46 sample. With the same edge tool kinematics, the D151 threshold stress lies at 42.4 MPa as has been found just recently, see in Sec. 8.

The influence of grinding kinematics was not taken into account in traditional strength investigations. At that time, specimens had been prepared very carefully in a special workshop. The results obtained with such samples now turn out to be somewhat optimistic for representing everyday practical cost optimized grinding processes. For D151, the traditional results match very well with that of the flat rotating tool results.²¹ Applying this kinematics can help improving strength compared with the rotating edge tool process. The gain for D151 from 42.4 MPa to 47.3 is $\sim 10\%$.

Nevertheless, the range of the threshold breakage stresses of D151, D64, and D46 prepared using the same kinematics is small with 42.4 to 51.0 MPa considering the maximum grain sizes differing by a factor of more than 3 (150 to 45 μm).

The maximum grain size of 49 μm of the SiC320 lapped sample is close to that of the D46 sample. The threshold breakage stress of 59.4 MPa of the SiC320 sample might mark the upper limit for D46 samples generated with a flat rotating tool. The close coincidence of the D25 and SiC600 samples supports this assumption. Their grain sizes are also quite similar if one assumes that for D25

the guaranteed value of 40 μm is much too conservative. The D25 sample has been prepared with a flat rotating tool.

The overall gain in strength using finer grains is not very high. From the coarse D151 grain to the fine grain D46, the increase of the threshold breakage stress is only 20%. With the use of microgrit grains of about 20 μm , maximum size strength gain of about 60% can be achieved. On the other hand, the threshold breakage stress values lie considerably higher than traditionally used values. Such values usually remained in the single digit MPa range. The threshold breakage stresses above 40 MPa thus represent an increase of more than a factor of four or even of seven for fine grains. This is a really significant improvement. However, it has to be borne in mind that these results are only valid for short-term loads. The transfer of the results to long-term loads where fatigue might play a role will be presented in the next section.

4 Fatigue—Stress Corrosion

4.1 Fatigue Mechanisms—Stress Corrosion

For loads lasting longer than some minutes up to many years, fatigue must be taken into consideration. The strength degradation of glass items has two main causes. One is worsening of the surface condition due to wear. Contact with harder materials in the form from bulky pieces to dust grains during use and cleaning processes lead to more and possibly deeper microcracks in the surface than were present originally. This fatigue effect can be reduced or even avoided by protecting the optical elements' faces for example by making them inaccessible or by covering them and by very careful cleaning. The other weakening cause is the growth of already existing subsurface microcracks under the influence of tensile stress. If tensile stress exceeds a threshold value, microcracks will start growing. Their growth starts with extremely low rate. If stress remains in this range, this so-called subcritical crack growth can go on for many years without leading to any breakage. The crack growth rate v depends not

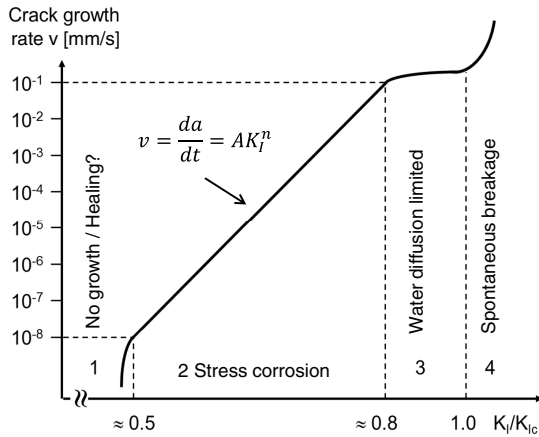


Fig. 6 Dependence of the microcrack growth on the stress intensity factor K_I .

only on stress σ but also on the crack's depth a and a crack form factor f . These three components combine to the stress intensity factor K_I , see Eq. (4). The index I , the roman numeral one, refers to the crack opening modulus one, which means just widening its cleavage. The two other modi, which exist in principle and are shear modi, are not present in glass.

With increasing stress intensity factor K_I , the crack growth rate follows an exponential law over many orders of magnitude see Fig. 6 and the following equations:

$$K_I = \sigma\sqrt{af}, \quad (4)$$

$$v = \frac{da}{dt} = AK_I^n. \quad (5)$$

K_I is the stress intensity factor, K_{IC} is the critical stress intensity factor, σ is the stress, a is the crack length, f is the crack form factor, v is the crack growth rate, n is the stress corrosion constant, and A is the crack growth parameter.

The crack growth rate reaches a plateau close to the critical stress intensity factor K_{IC} , which is also called fracture toughness. After the plateau at K_I approaching K_{IC} , crack growth speeds up drastically with ending in breakage within very short time.²²

The presence of water enhances the growth of microcracks under tensile load. It does not need to be liquid water; humidity alone has a significant effect. Water molecules entering the microcracks and drifting to the tip facilitate ripping atomic bonds of silicon and oxygen apart. These bonds are the basic elements of most common glass types. Glass loaded in dry environment especially in vacuum has the lowest fatigue effect. The stress corrosion constant n enters the crack growth law [Eq. (5)] as exponent. Environmental humidity is a huge influence on long-term strength. At the plateau, range 3 in diagram 6 the crack tip moves faster than water can follow thus making the growth enhancement ineffective. For long-time applications, it is important to remain in the lower range of crack growth rate.

4.2 Measurement of the Stress Corrosion Constant

There are several methods available for measuring the stress corrosion constant n . One is to observe the growth of a single

Table 1 Stress corrosion constant n for ZERODUR® under different environmental conditions from three measurement campaigns. The numbers in brackets give the environmental relative humidity.

Method/ Humidity	Ground samples ring-on-ring setup load rate variation	Ground samples ring-on-ring setup load rate variation	DCDC
Dry	79.1 (N ₂ ; 5-ppm residual water)	—	50 ± 3 (3%)
Normal	31.1 (50%)	29.3 + 3.6/ -2.9 (50%)	31 ± 3 (37%)

crack directly with increasing stress intensity factor K_I using a microscope. Another method is the dynamic breakage stress method. Samples of tiles with ground surfaces are loaded with different stress increase rates. The setup is of the same ring-on-ring type as described before in Sec. 3. The relative shifting of the samples allows deriving the stress corrosion constant. Since the surfaces analyzed with this method are the same as those used in practice and in the investigations presented above, this method was the preferred one.

The stress increase rate applied for determining the stress corrosion constant of ZERODUR® varied over four orders of magnitude in order to achieve a wide range of validity, especially also for longer lasting loads. The rates of 40 to 0.0040 MPa/s correspond to time until breakage extending from 1.5 s to 3.5 h. The measurements were done in normal ambient humidity environment and in extremely dry nitrogen environment with 5-ppm residual water content. Ideally, the median strengths of the samples if plotted against the stress increase rates on logarithmic scales render a straight line. The stress corrosion constant n results from the slope of the straight line fitted to the data.²³

Table 1 displays the stress corrosion constant values for ZERODUR® obtained in three-different measurement campaigns. In column 2, the measurement results described above are summarized. The value in column 3 derives from earlier measurements with a narrower span of stress increase rates and column 4 provides values obtained using a method called double cleavage drilled compression (DCDC). This is a direct observation method of cracks starting to grow from ground surfaces.²⁴ The values for normal humidity of all three measurements match each other very well. Therefore, the value $n = 31$ is considered to be well-established for normal humid environment. For application under very dry earth-bound application, one can choose $n = 50$ and in vacuum $n = 79$ is adequate.

Fatigue occurs only under external influences. As long as a glass item is stored protected against mechanical damages and without being subject to a considerable stress load no degradation of its strength will occur.

5 Increasing Strength of ZERODUR® Surfaces with Etching

5.1 Methods for Strength Increase

There is a variety of methods for increasing strength of glass items. One way is to introduce compressive stress into the

surface. It acts as a hurdle for tensile stress, which has to be overcome before tensile stress starts the growth of microcracks. This can be achieved by thermal or chemical prestressing. Another one is to protect fire polished surfaces in between laminated glass sheets as it is done for car windshield panes. These methods are not suitable for precision optical elements. The only possible way is to reduce the depths of the microcracks or at best to remove them completely. Finer grains used for grinding or lapping reduce the depths. Polishing can push this much further. A complete removal of microcracks can be achieved by etching.

A considerable gain in strength by etching requires a minimum layer thickness to be etched off.²⁵ This is approximately equal to the maximum microcrack depth. Such an etching process employs very strong acids requiring special equipment and safety precautions. After etching, there will be no sharp crack tips left over. However, the surface texture is not as flat as it is the case for polished surfaces. It represents more a layer of micropits touching each other and forming ridges and tips (see Sec. 6). This makes the surface of etched items touch sensitive with the risk of reducing the strength gain again. Etching of ZERODUR® has been applied successfully in a number of astronomical projects and it is increasingly important for future projects such as the ESO ELT.

5.2 Measurement Results

In order to learn more about the possible strength gain for etched ZERODUR® surfaces and the related conditions, samples with etched tiles have been measured together with the just ground samples from the very beginning of the measurement campaign since 2007. Figure 7 shows the breakage test results for ZERODUR® first ground and then etched in a Weibull plot.²⁵ For reference, it also contains

the two samples of the only ground surfaces D151 (coarsest) and D25 (finest), which define the range of ground surface breakage distributions for ZERODUR®. The denominations in the format DXXXEYYY indicate the last grinding step with a diamond tool with the grain size specification DXXX. The EYYY represents the etched off layer thickness in μm . For example, D151E123 means D151 ground surface with a layer of 123 μm etched off subsequently.

The measurement of all samples with etched surfaces began with an original number of about 150 tiles for each sample. The higher the strength is the more tiles break starting from a location outside the load ring area and thus will be discarded from evaluation. The table in Fig. 7 lists the number of regularly broken specimens N_v and the minimum and maximum values found.

The lowest data points of all distributions for etched surfaces except one lie higher than 125 MPa. The exceptional distribution D151E34 with only 34- μm layer thickness etched off, lies very close to the only ground distribution. This shows clearly the need to etch off a minimum layer thickness in order to reach considerable strength increase. The layer etched off must have a thickness close to or larger than the maximum microcrack depth of the preceding grinding process. This is about 50 μm for D64 and 110 μm for D151.

Samples with layer thickness etched off close to or even somewhat smaller than the maximum microcrack depth (D64E73 and D151E83) show continuous distributions with a shape close to that of three-parameter Weibull distributions. With larger etch depth distributions shift to higher breakage stresses, the D151 deeper etched samples (D151E123 and D151E181) lie considerably higher. However, the additional 60 μm taken off with D151E181 do not result in a significantly higher breakage stress. Both samples lie very close to each other. Moreover, both in

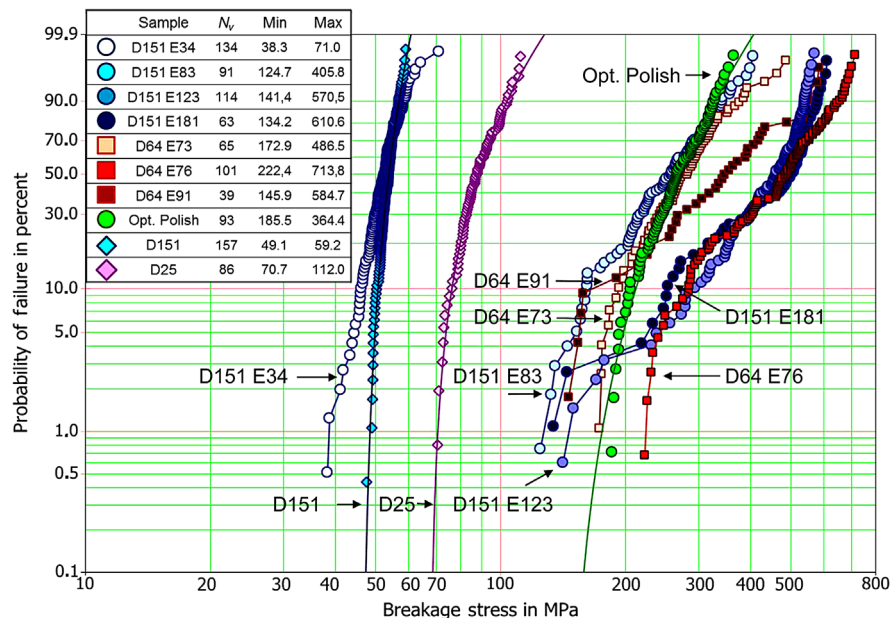


Fig. 7 Samples of ZERODUR® specimens first ground and then etched (squares and circles). For reference, the diagram contains two ground surface samples (diamonds) D151 (coarse grain) and D25 (fine grain) and the sample of optically polished ZERODUR® (green circle). Opposite to the etched surface samples the ground and polished tiles' samples follow a three-parameter Weibull distribution very well.

common divide into two ranges. The continuous series of data extend down to about 220 MPa. Below this value both samples show some few isolated data points, which could be considered as outliers. The deeply etched D64E91 sample looks similar. The D64E76 sample deviates from this general behavior at first sight. However, most of its data points match with those of the deeply etched D151 samples. Again the continuous data series goes down to about 220 MPa, but here outliers are missing. The other end of the distribution reaches the highest breakage stress values of all.

For samples with etched specimens, the three-parameter Weibull distribution does not fit the data reasonably. The reason is that there are at least two breakage mechanisms. One is breaking from weak spots in the etched and otherwise untouched and visually flawless surface. Such breakages occur at stresses higher than 200 MPa extending up to 700 MPa. Type and size of the breakage origins are not known. The other mechanism is breaking from microdamages introduced after etching. These are again microcracks with sharp tips but very small depths, see Sec. 6. If the microdamages could be prevented also etched surface samples might follow the three-parameter Weibull distribution. The sample of optically polished ZERODUR® supports this hypothesis. With polished surfaces being extremely flat and free from pits, ridges, and tips, it is not prone to microdamages. The sample follows the three-parameter Weibull distribution indeed, see Fig. 7.

Just as with ground surfaces the very important question for etched surfaces is: is there a maximum microcrack depth and as a consequence is there a minimum breakage stress? The argument in favor of the existence is that the breakage data of all samples with deeply etched surfaces lie above 220 MPa with the vast majority of their data points (D151E181, D151E123, D64E91, and D64E76). It can be assumed that above this value breakage starts from pristine etched surfaces. The origin type is not known up to now. Sharp tip cracks are not present anymore. It will be very difficult to investigate the breakage origins. They are expected to be smaller than 1 μm . This follows from the observed breakage stress range from 220 up to 700 MPa for etched surfaces in comparison with ground D25 and lapped SiC600 surfaces. Here breakage stresses vary between about 70 and 130 MPa with maximum crack depths being below 20 μm extending probably into the single-digit range. Additionally, breakage origins in etched surfaces are very rare. The fact that many tiles break from outside of the load ring indicates that in such cases within the load ring there was no flaw capable to start breakage even at stress values of many 100 MPa. For a given stress level, there can be several square centimeters without any origins capable to start breakage. Thus their number per area is very low compared with the microcracks in ground surfaces. The number drops from more than 10,000 microcracks per cm^2 for ground surfaces down to 1 or even less breakage origins for etched surfaces per cm^2 . The much broader breakage stress distributions of etched surfaces support this conclusion. If many breakage origins per area existed, the steps between two neighboring data points should be much smaller.

Below 220 MPa, there are some isolated data points from the deeply etched samples, which most probably come from

microdamages introduced after etching, see Sec. 6. Etched tiles' surfaces have a micropit layer, which is sensitive against careless handling. The resulting microdamages had not been realized before. The samples with less deep etching (D151E83 and D64E73) extend down to breakage stress below 220 MPa continuously without any obviously isolated data points. D64E73 still lies quite high with a minimum breakage value measured at 173 MPa, D151E83 goes down to 125 MPa. This gives reason to assume that there are some residual flaws present, which have not been removed by etching completely. The failure probabilities for both samples drop sharply indicating a minimum breakage stress value to exist in each case. In all samples, microdamages might be present. A characterization of their depth distribution is not possible because their generation is an undefined process. However, also with these damages, a minimum breakage stress can be assumed. The peak to valley range of the pits is limited, which again limits the possible crack depths.

Some even lower lying data points of some samples in Fig. 7 have been eliminated as outliers. They come from deep scratches in the tiles' surfaces of different origins. Data points representing different breakage origins such as from pristine etched surfaces, from microdamages and from deep scratches must not be put together into one sample for statistical evaluation. Fitting such samples with one statistical distribution for the purpose of breakage probability extrapolations is not possible. For this reason, the fit of any distributions to etched samples has been omitted even though for the samples with lower stress tolerances the three-parameter Weibull distribution does fit. However, this would be pure mathematics without physical justification.

The argument against the existence of a minimum breakage stress is the existence of outliers, which could not be proven to be outliers by clear evidence. Part of that comes from a poor documentation, which had not been deemed to be necessary at the time, when the experiments had been performed. This is part of the lessons learned.

From the presented evidence, the existence of a minimum breakage stress for etched surfaces is proven. Experience from applications supports this finding. Etched ZERODUR® structures have been tested and used successfully with short-term high loads with the LISA Pathfinder project.^{3,26} Examples for long-term applications of deeply etched structures are the 1-m diameter extremely lightweighted secondary mirrors of the Gemini telescopes. They are loaded by rapid tip-tilt and chopping mechanisms since their first light in 1999.²⁷

The data presented in Fig. 7 indicate that the minimum breakage stress of deeply etched and untouched surfaces lie at about 220 MPa. For practical use, this is too optimistic. It is better to accept some degradation due to possible microdamages. Even for moderately deep etched surfaces and for outliers of deeply etched surfaces, no value has been found lower than 125 MPa. Therefore, the assumption of a minimum breakage stress at 120 MPa for short-term loads is conservative. However, it has to be emphasized that just as with ground surfaces it is essential that the high-strength surface condition is not degraded by the introduction of any deeper flaws neither by careless processing of the surfaces before etching nor by inadequate handling after etching.

6 Microcracks—Depths and Removal by Etching

6.1 Subsurface Microcracks and Roughness

Subsurface microcracks occur during surface generation of glass and glass ceramic. Figure 8 shows an optical micrograph of the cross section of a ZERODUR® D151 ground surface along a length of about 2 mm. The roughness range of about 25 μm is clearly visible as well as frequent deeper microcracks. Microcracks extend deep into the bulk material see Figs. 8 and 1. Therefore, the surface roughness measurement is not sufficient for determining microcrack depths. A mechanical tactile stylus cannot follow them, because the cleavages are too narrow. The expression “sub-surface microcracks” emphasizes the distinction to surface roughness.

The good workshop practice for removal of subsurface damages is to take off a layer with a thickness at least 3 times larger than the maximum crack depth of the preceding process. In order to achieve strength-enhanced surfaces, a layer at least as thick as the maximum crack depth has to be etched off. For these purposes, it is necessary to know the maximum microcrack depths caused by grinding with different tools and processing parameters.

6.2 Maximum Microcrack Depth

There are several investigations of microcrack depth distributions applying different methods for observing crack

depths.^{28–31} At SCHOTT, the following method is used frequently. Specimens are ground with different diamond grain tools or lapped with silicon carbide. Breaking them from a narrow groove ground in the back side provides edges enabling crack observation with a microscope as shown in Fig. 8. The measurement result is a frequency distribution of crack depths per observed length. Figure 9 displays examples of such distributions for ZERODUR® from investigations done by SCHOTT.³²

The observed depths of microcracks are not equal to the full breakage effective depths. The only nanometer wide cleavage at the tip makes this part of the crack invisible. Additionally, the zero line is not well defined due to surface roughness. At small crack sizes, the depth determination is limited additionally by larger cracks partly obscuring the smaller ones.

Generally, the microcrack depth frequency drops exponentially. This makes crack depths larger than the observed maximum crack depth very improbable and supports the existence of a maximum microcrack depth in practice.

Figure 10 comprises investigation results for the maximum crack depth plotted against the maximum grain size of the diamond grains of different grinding tools. They have been obtained partly with different observation methods. The line fitted to the data of SCHOTT Strothotte 1991 is a good representation of the relationship between the two quantities. These data cover the widest range of grain sizes. At smaller grain sizes, other investigations

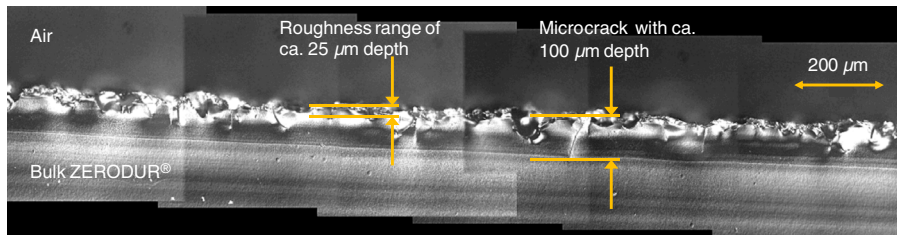


Fig. 8 Optical micrograph of the cross section of a ZERODUR® D151 ground surface, along a 2-mm edge.

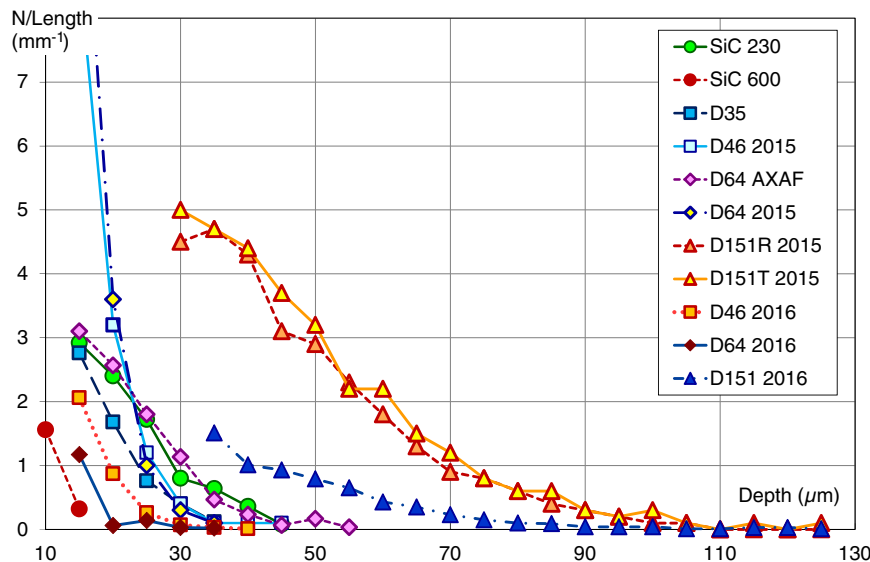


Fig. 9 Microcrack depth distributions in ZERODUR® ground or lapped with different grain sizes. R and T refer to observation in directions parallel and perpendicular to tool marks, respectively. AXAF indicates data obtained on occasion of the CHANDRA/AXAF project.

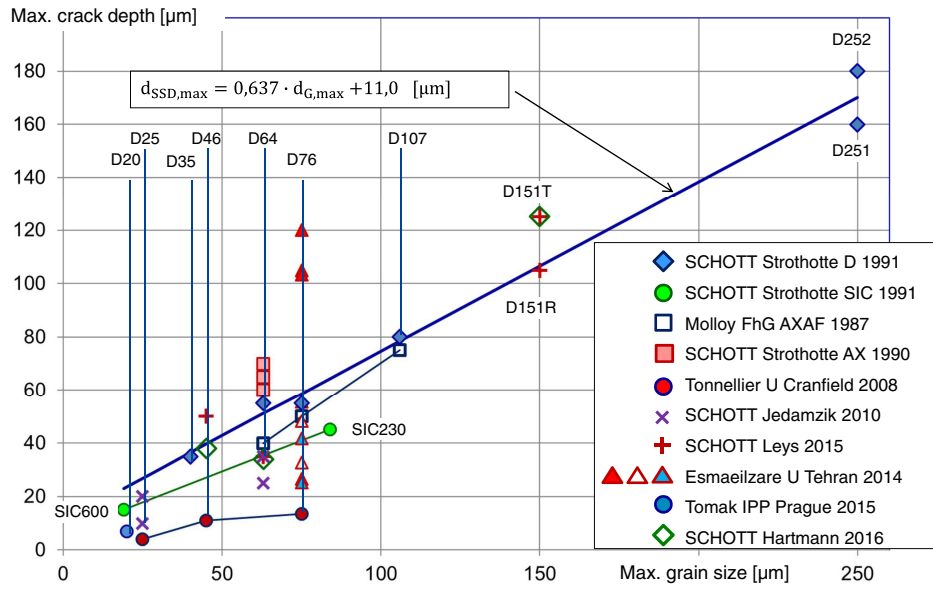


Fig. 10 Maximum crack depth in ZERODUR® surfaces prepared with different grain sizes and types (bonded diamonds D and loose SIC lapping grains) specified by their maximum grain size. The straight line is a fit to the “SCHOTT Strothotte D 1991” data set.

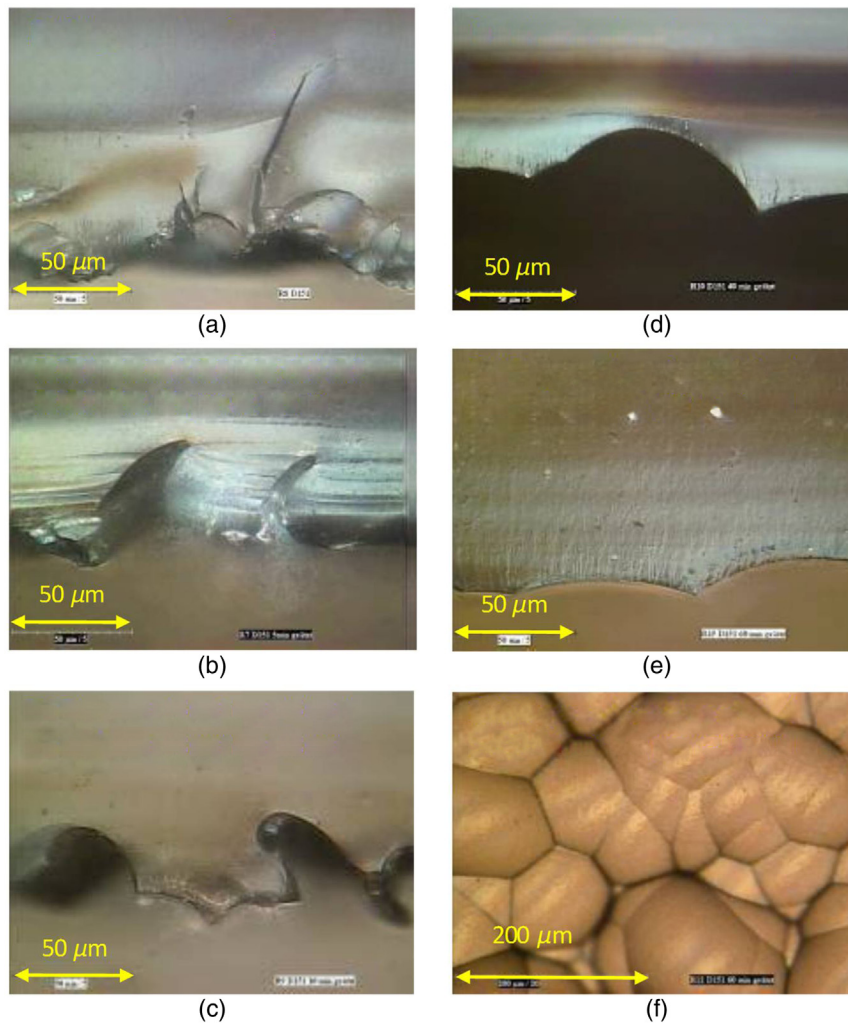


Fig. 11 ZERODUR® ground with (a) D151 diamond grain tool as ground surface, and etched for (b) 5 min for 20-μm removal, (c) 10 min for 38-μm removal, (d) 40 min for 108-μm removal, (e) 60 min for 158-μm removal, and (f) top view of (e).

tend to smaller maximum crack sizes. Data points at D76 deviating upward come from grinding processes with unusual harsh tool movement, which is not used in common manufacturing. The data from Tonnelier²⁹ show that with special processes considerably lower depths are achievable.

6.3 Microcrack Removal by Etching

Figure 11 shows cross sections and a top view of a ZERODUR® surface ground with a D151 diamond grain tool in different stages of etching: as ground, and after 5, 10, 40, and 60 min etching with SCHOTT standard acid. After 10 mins of etching and removal of 38- μm layer thickness, cracks are still visible but with rounded tips. From the breakage testing of a D151 sample with 34 μm etched off, one knows that such surfaces are not stronger than the only ground samples. It needs the arc-like topography formed throughout the surface to achieve considerable strength increase [see Fig. 11(d)–(f)]. This is the case after 40 min of etching with 108- μm etched off, a value that is just the maximum crack depth for D151 according to the correlation line of Fig. 10. Further etching smoothens, the arcs become wider and shallower as shown in the images of 60 min etched ZERODUR® (cross section and top view). All microcracks introduced by the grinding tool are removed resulting in a reliable strength gain. Consequently, further etching does not lead to considerable additional strength gain but only to a topographical change of the arc structure

6.4 Microdamages

Microscopic pictures of surfaces from etched tiles, which have broken at stresses higher than 450 MPa show smooth arcs without any damages, see Fig. 12(a). There are no obvious breakage origins present.

Within the breakage stress range between 120 and 450 MPa, etched specimens have been observed to acquire tiny damages after etching, so-called microdamages [see Fig. 12(b) and Ref. 33]. These damages occur at vulnerable ridges and tips [see Fig. 12(c)] possibly just from careless touching of the surface. Due to the small surface height variation of a few micrometers, the microdamages are tiny. The crack depths remain in the single-digit micron range and the breakage stresses above 120 MPa.

Most recent investigations on scratching of etched ZERODUR® surfaces support this observation. Enhanced effort was necessary to create deeper scratches.³⁴

The creation mechanism of the microdamages in etched surfaces is undefined, since contact materials, forces, duration, repetitions, and other possible influences are not known and will vary case by case. It is to be expected that in the lower part of the breakage stress distributions of Fig. 7 breakages can start either from a microdamage or from the pristine etched surfaces breakage origin. For this reason, one cannot expect breakage stress to follow a unique statistical distribution. The failure of fitting a Weibull distribution to such data is not surprising.

7 Lifetime Calculation

7.1 Higher Loading of Glass Items

There is a general reluctance against mechanical loading of brittle glass or glass-ceramic items. The proverbial tendency to breakage, its sudden occurrence, and the total damage in many cases combined with the creation of razor blade sharp edges quite often prevent even considering the application of glass. On the other hand, it is used ubiquitously because of its unique properties such as its transparency, its beauty, and its optical properties. Common day experience shows that many glass items work for many years without any breakage thus justifying their use. This supports the hypothesis that there is a minimum strength and a potential for higher loading of glass. However, in order to exploit this, some obstacles have to be overcome.

The traditional failure probability calculation based on the two-parameter Weibull distribution predicts finite failure probability even for arbitrarily low bending stress.³⁵ In this approach, the first question in strength design to be answered is, which failure probability is acceptable? Hardly anyone likes to provide a specific number. The second and third questions relate to the size of the loaded area and the fatigue to be assumed. Usually at each stage, the considerations made are conservative or even over-conservative. In the end, this adds up to a factor of safety, which is much too large. The admissible stress will be reduced to minute values. They will be hardly higher than the conservative rule-of-thumb values of 4 to 6 MPa for glass items and 10 MPa for glass-ceramic items. Even for these values, failure probabilities different from zero exist. This approach did not increase the number of glass applications with higher mechanical loads. It prevented promising use instead.

One important criterion for strength design is the damage consequences. For cheap and easily replaceable glass items such as drinking glasses, one will not make any subtle design

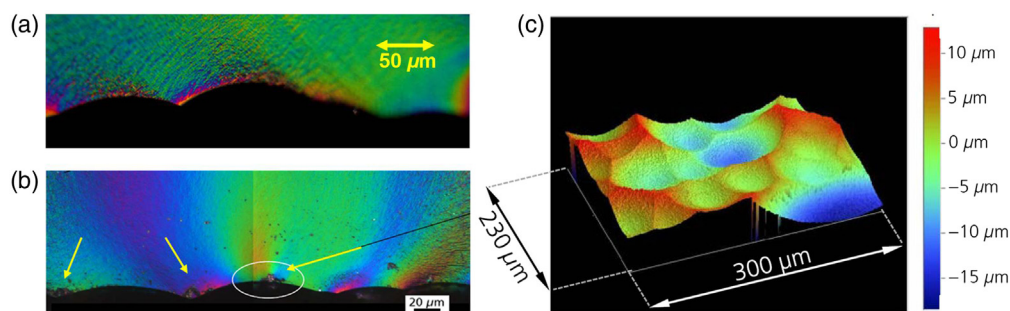


Fig. 12 Optical micrographs of etched ZERODUR® (false-colored): (a) and (c) surface topography of etched with pits, ridges, and tips, and (b) microdamages at an etched surface. Images provided by the Fraunhofer Institute for Mechanics of Materials IWM in Freiburg, Germany.

considerations even when they are exposed to higher loads, for instance by thermal stress. For high-value items such as astronomical mirrors or safety relevant items such as windows of manned space crafts, things are different. No matter which design calculation method will be applied for such items, in the end, they are subject to a proof test.³⁶ Loading the item somewhat higher than planned will guarantee its integrity during application after passing the test. Below the admissible stress, the item will react deterministic on any loads. Unfortunately, this method is time consuming and expensive.

The strength design method based on the threshold stress of the three-parameter Weibull distribution presented below provides the same highly valuable advantage as the proof test. This is the admissible stress up to which the glass items behave deterministic. An area dependency as with the two-parameter Weibull approach does not exist and fatigue is incorporated in an elegant and reliable way. The disadvantages are also very similar. A proof-tested item must not be touched or even scratched anymore. The surface of a three-parameter Weibull threshold designed item must be the same as those for which the threshold had been determined. Any additional surface flaws are not allowed. However, there are ways to achieve this in practice such as covering critical surfaces or making them inaccessible.

7.2 Lifetime Calculation with the Weibull Threshold Stress Model

The lifetime calculation using the Weibull threshold stress model for a ZERODUR® item subject to a constant load is based on the following considerations. For a ZERODUR® item with a well-prepared surface without additional damages such as scratches or chips, a threshold breakage stress exists below which the breakage probability is zero (see Sec. 3). It is possible to determine the threshold breakage stress by breakage stress measurement. The minimum number of specimens allowing fitting of the three-parameter Weibull distribution is about 50 with the more the better.

In measurements, using the stress increase rate of 2 MPa/s loads last from half a minute for ground surfaces up to several minutes for etched surfaces to break. Therefore, the obtained threshold breakage stress is valid only for short load duration. The crack growth law presented in Sec. 4 allows taking account of fatigue for long-lasting loads with duration up to many years. The stress corrosion constant ruling fatigue is available for several typical environmental humidity conditions for ZERODUR® applications. Integration of the crack growth law Eq. (4) for constant stress and again for constantly rising stress leads to the lifetime $t_{B,c}$.³⁷

$$t_{B,c} = \frac{\sigma_{B,r}^{n+1}}{\sigma_{B,c}^n (n+1)\dot{\sigma}_r} \frac{1}{\sigma_{B,c}} \quad (6)$$

$\sigma_{B,c}$ is the constant stress load or required design strength respectively, $\sigma_{B,r}$ is the breakage stress measured with constant stress increase, $\dot{\sigma}_r$ is the constant stress increase rate during measurement (2 MPa/s), and n is the stress corrosion coefficient characterizing the fatigue effect.

Inserting the experimentally determined threshold breakage stress σ_T for $\sigma_{B,r}$ results in the minimum lifetime before the first breakage will occur [see Eq. (7)]. Solving this

equation for $\sigma_{B,c}$ results in the allowable constant stress for a required minimum lifetime [see Eq. (8)]

$$t_{B,c} = \frac{\sigma_T^{n+1}}{\sigma_{B,c}^n (n+1)\dot{\sigma}_r} \frac{1}{\sigma_{B,c}} \quad (7)$$

$$\sigma_{B,c} = \left[\frac{\sigma_T^{n+1}}{t_{B,c} (n+1)\dot{\sigma}_r} \right]^{\frac{1}{n}} \quad (8)$$

In Fig. 13, the lifetime of ZERODUR® items is plotted against the applied constant stress for the stress corrosion constant $n = 31$, which is valid for normal environment with 50% relative humidity. Five curves represent different ZERODUR® surface conditions: ground with diamond tools D151, D46, D35, and D25 (from left to the right). The D64 tool threshold stress is very close to that of D151, so the D151 curve also holds for D64. The fifth curve represents ZERODUR® first ground and then acid etched. The curve “etched” is based on a minimum breakage stress value of 120 MPa. This presupposes that the etched off layer is at least as thick as the maximum crack depth of the preceding grinding process. It is justified to use the crack propagation model as presented in Sec. 4 since at 120 MPa up to about 200 MPa breakage origins will be microdamages with sharp tips. The value 120 MPa is smaller than the lowest experimentally found value for any etched surface and thus it can be considered as conservative. For the etched condition curve, three examples demonstrate how to read the diagram: 70.2 MPa is the highest allowable constant stress for etched ZERODUR® with 120 MPa short-term strength, when it is required to survive at least one year in normal humid environment without breakage. At constant stress of 65.1 MPa, it will endure 10 years and at 61.8 MPa for 50 years. This prediction requires that no surface degradation will happen except for the microcrack growth under tensile load. The surfaces must be free from deeper microcracks than those generated by the grinding and etching process. Additional wear such as abrasion and damages during operation is not allowed.

Figure 14 displays minimum lifetime curve sets for three different surface preparations (ground with a coarse D151 diamond grain tool, ground with a fine microgrit D25 diamond grain tool as well as ground and subsequently etched). For each of them, three curves are plotted for different environmental humidity conditions (in each case from left to right: normal 50% relative humidity with stress corrosion constant $n = 31$, very dry desert $n = 50$, and extremely dry vacuum $n = 79$). Figure 14 shows the high gains for breakage stress design, which the presented method enables. ZERODUR® items with coarse ground D151 surfaces withstand about 25 MPa for 10 years in normal humidity environment before the first breakage will occur. In vacuum, the allowable stress for D151 and 10 years rises to 36 MPa for D25 surfaces to even 51 MPa. Comparing different curves for the same surface preparation at the same tensile stress demonstrates the huge influence of environmental humidity. For example, etched surfaces with short-term minimum breakage stress of 120 MPa will break within several hours in normal humidity if loaded with 90 MPa, in dry environment, they will survive about one month and in vacuum more than 50 years.

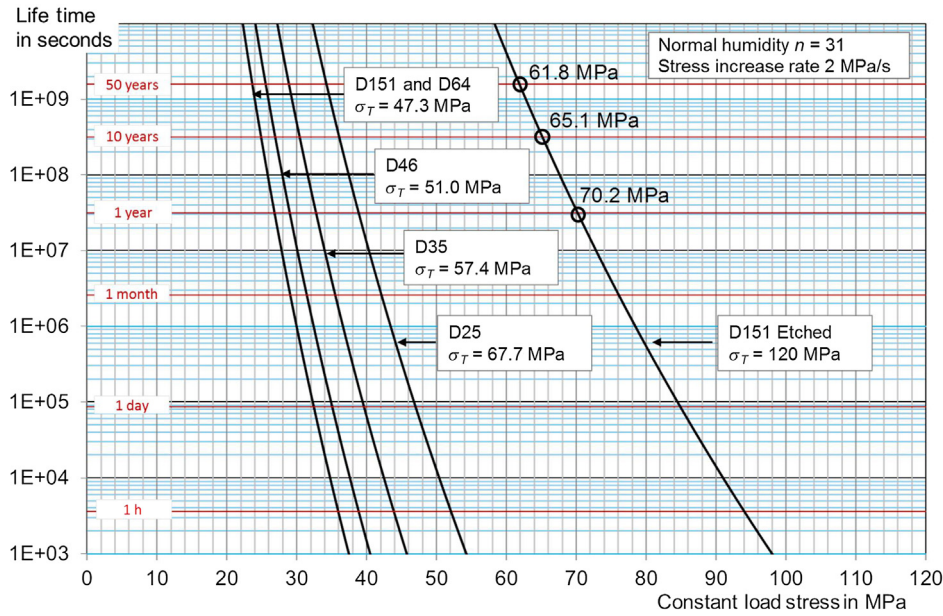


Fig. 13 Lifetime calculations of ZERODUR® items prepared with five different grinding tools D151, D64, D46, D35, D25, and ground and then etched in normal humidity environment ($n = 31$). The D64 and the D151 ground surfaces curve are the same because the threshold stress values are almost identical. The short-term threshold stresses for the ground surfaces used for the calculations are given in Fig. 5. The short-term minimum breakage stress for the etched surface curve is 120 MPa. This holds for a surface with a layer thickness etched off greater than the maximum crack depth introduced by the preceding grinding process.

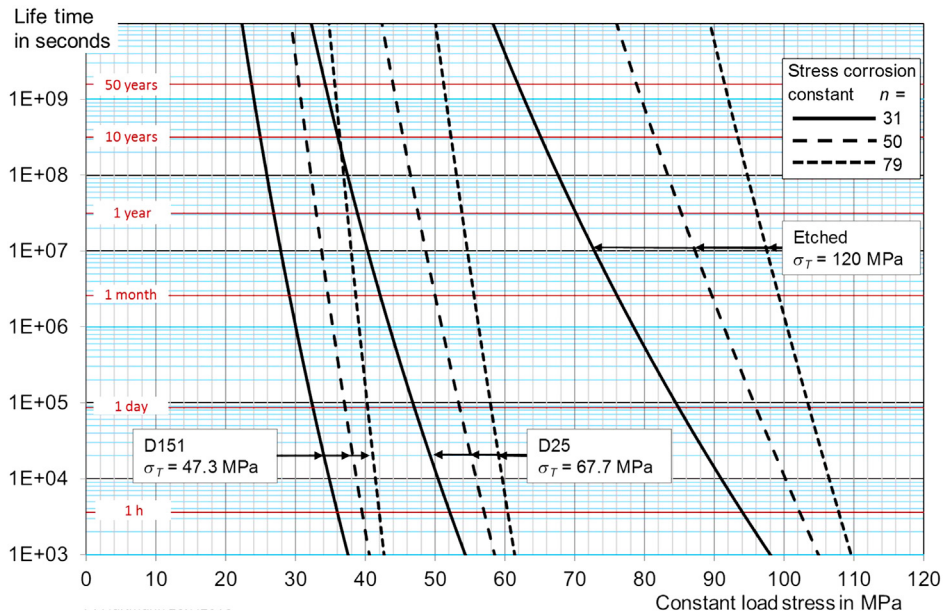


Fig. 14 Lifetime calculations of ZERODUR® items prepared with two different grinding tools D151 and D25, and ground and then etched in three different humidity environments. For each surface condition from left to right: normal 50% relative humidity $n = 31$, dry desert climate $n = 50$, and extremely dry or vacuum $n = 79$.

8 Lifetime Calculation—Test of the Model

The Fraunhofer Institute for Mechanics of Materials IWM in Freiburg, Germany, is equipped with a set of ring-on-ring test setups allowing applying constant loads for long-time periods. This provides an opportunity for checking the validity of the lifetime calculation model outlined in Sec. 7.2.

ZERODUR® D151 ground tiles were kept at three different constant loads (30, 34, and 38 MPa) until they broke. The lifetimes of all tiles are expected to be higher than those predicted by the model. The tiles had been prepared employing a disk tool with grinding at its circumferential edge moved from the edge to the center of a 1.5-m diameter rotating disk.

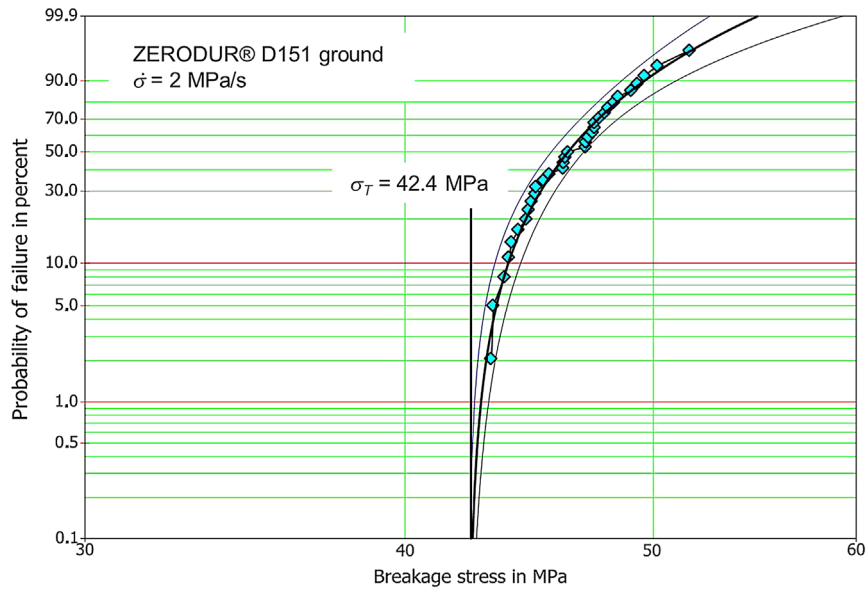


Fig. 15 Threshold stress analysis of a ZERODUR® D151 disc edge tool ground and measured with 2 MPa/s stress increase rate. σ_T indicates the three-parameter Weibull threshold stress.

This arrangement which is sometimes used for faces without load requirements turned out not to be best suited for strength optimization. It generated scratches from grains getting isolated and breaking off during the grinding process. Some atypical surface imperfections and thus outliers had to be expected.

Figure 15 shows the results of a sample of 33 specimens dynamically broken with the stress increase rate of 2 MPa/s with the same method as outlined in Sec. 3. It serves for determining the threshold stress, which was found to be 42.4 MPa. Two data points at 37.5 and 40.6 MPa have

been removed as outliers. Inserting this value into Eq. (7) together with the 2 MPa/s stress increase rate and the stress corrosion constant of 31 for normal humid environment, the lifetime curve is calculated (see Fig. 16.) All data points are expected to lie above the lifetime prediction curve. Three data samples are available. For the constant loads of 38 and 34 MPa, all tiles have been kept in the setups until they broke. For the 30-MPa sample, the measurements were stopped after 7 days in order to not occupy the setups too long. Some tiles might have survived much longer than one month. Therefore, this sample is truncated upward.

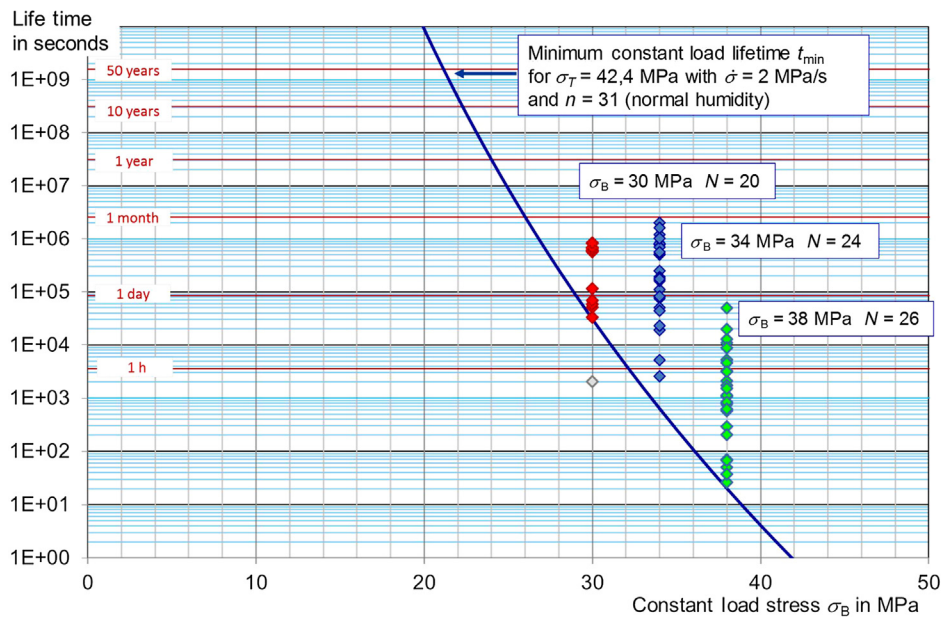


Fig. 16 Lifetime of D151 ground ZERODUR®. Comparison of the lifetime prediction curve according to Eq. (7) obtained with the parameters given in the diagram and experimental lifetimes of tiles loaded in double ring test setups with three-different constant tensile stresses (30, 34, and 38 MPa) until breakage. The 30-MPa constant load sample is truncated upward. Tiles surviving 7 days have been removed for releasing measurement capacity.

The minimum lifetimes predicted are 20 s (38 MPa), 10 min (34 MPa), and 8 h 22 min (30 MPa). These values do not represent very long-time applications such as months or years but they cover a range of more than three orders of magnitude.

The results are depicted in Fig. 16. From the 70 specimens in total, 69 fulfil the requirement to lie above the minimum lifetime curve. One data point of the sample subjected to 30 MPa constant load lies below. A closer inspection of the broken tile did not show an obvious exceptional cause for the low breakage. However, such cause can also not be excluded completely. Nevertheless, the overall result supports strongly the validity of the presented lifetime calculation method based on the threshold breakage stress. In an earlier publication,¹⁰ the sample with 2 MPa/s stress increase rate was not available. The existing sample with 40 MPa/s stress increase rate did not lead to a fitting lifetime curve. The cause assumed was that fatigue works too slowly for such fast breakages. For the low increase rate of 2 MPa/s, providing sufficient time for fatigue to become fully effective a threshold stress of 42 MPa was predicted, which is now verified clearly.

The presented lifetime calculation model enables predictions with precision unprecedented in brittle material strength. It removes uncertainty considerably and opens up new application possibilities for these materials. Moreover, it is not restricted to ZERODUR®. A minimum breakage stress will be present in each brittle glass and glass-ceramic item. It is to be expected that for a considerable set of applications it should be worthwhile to put some more effort in

determining the threshold breakage stress values for typical surface conditions and the fatigue parameter, the stress corrosion constant for the given material and its intended environment.

9 Application Examples

The satellite mission project LISA Pathfinder, which initiated the ZERODUR® strength measurement campaign 10 years ago, is an example for a high-level short-term load. ZERODUR® is used as material combining extreme dimensional precision with mechanical robustness see Fig. 17. The successful launch in December 2015 and the following gravitation test mass measurements have confirmed the suitability of the material for such demanding applications.

ZERODUR® has been and is used in a considerable number of space applications.³⁸ Some of the ZERODUR® elements had not only to survive launch accelerations. The spinning and scanning movements of the METEOSAT second generation imaging systems loaded the employed ZERODUR® mirrors for many years continuously [see Fig. 18(a)].

Wobbling loads act on the secondary mirrors of the GEMINI 8-m class telescopes since now 20 years, see Fig. 18(b).

Very long-lasting loads will act on ZERODUR® mirrors of the European ELT. Each of the 931 M1 mirror segments will be bonded at more than 20 spots to warping harnesses not only for support but also to apply for continuous shape optimization (see Fig. 19). These bonds shall endure the 50 years planned lifetime of the telescope.

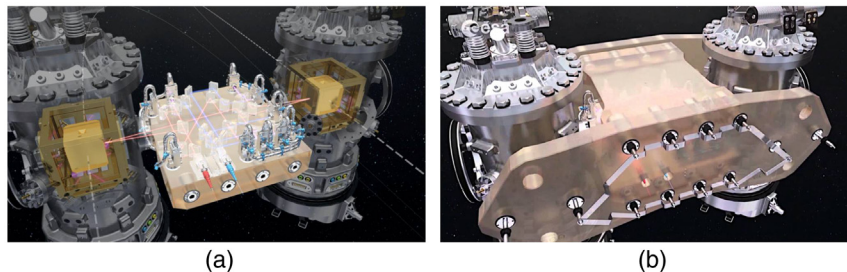


Fig. 17 LISA Pathfinder ZERODUR® components: (a) optical bench and (b) support frame for test mass containers. © ESA.

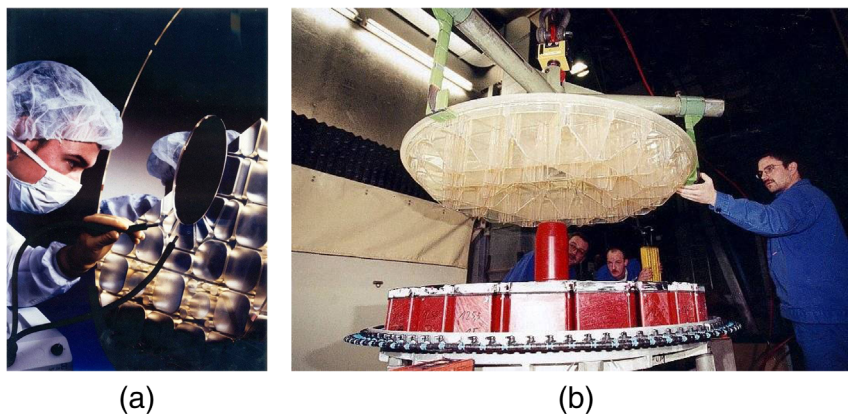


Fig. 18 Photographs of (a) METEOSAT Seviri ZERODUR® scanning mirror © Carl Zeiss and (b) GEMINI 8-m telescope secondary mirror.



Fig. 19 Photograph of the European ELT ZERODUR® M1 mirror segment on warping harness. © ESO.

10 Conclusion

Investigations since 2007 and successful projects have proven the suitability of the extremely low-expansion glass ceramic ZERODUR® for applications with considerably higher mechanical loads (30 to 100 MPa) than accepted before.

Just as with all brittle cast materials, the presence and depth of subsurface microcracks are the decisive influences on tensile strength. For mirror and support structure faces, which are generated in optical workshops according to good manufacturing practice, microcracks do not extend arbitrarily deep. A maximum microcrack depth for each surface preparation exists depending on the grinding or lapping grain size as well as on the grinding process itself.

In breakage stress measurements, the maximum microcrack depth is reflected by the existence of a threshold breakage stress. The breakage stress results for the investigated ZERODUR® samples follow the statistical three-parameter Weibull distribution. Below the threshold stress failure probability is zero and reactions on loads can be treated deterministic.

The fatigue effect of subcritical microcrack growth under tensile stress is well understood. It is characterized by the stress corrosion constant, which is known reliably for ZERODUR® for the main important environment conditions normal humidity, dry and extremely dry.

The considerably enlarged data basis on breakage stress samples allows calculating lifetime including the fatigue effect. Using the threshold stress allows calculating minimum lifetimes excluding any earlier breakages. This holds for surfaces without additional scratches and flaws, which are not typical for the surface preparation. Long-term measurements checking the validity of the minimum lifetime calculation method support the approach.

Etching of ground surfaces increases strength up to 120 MPa or even higher for short-term loads. This presupposes that a layer is etched off with thickness equal or larger than the maximum crack depth induced by the preceding grinding process. Due to their topography, etched surfaces are sensitive against touching eventually causing microdamages. They remain very small and thus do not reduce the strength of etched surfaces below 120 MPa. Avoiding such microdamages can raise strength much further. In any case, this requires the absence of any later introduced deeper cracks. Samples with etched surfaces do not necessarily follow a three-parameter Weibull distribution since

the condition that only one breakage origin mechanism exists is not assured. If breakage stress of specimens originating from pristine etched surfaces will follow the three-parameter Weibull distribution or not, cannot be concluded from the existing data sets. This requires measurements with specimens free from microdamages.

The breakage stress threshold-based lifetime method provides considerably better reliability together with higher possible mechanical loading of glass and glass-ceramic items than methods used before. With careful evaluation of given surface conditions, it can be used with other glasses and glass ceramics in a much wider field of applications than presented here.

Acknowledgments

The author thanks Günter Kling and Stefano Lucarelli from company Airbus Defence and Space, Friedrichshafen Germany, for starting and supporting the measurement campaign, Oliver Sittel, Eugen Kürner, Thomas Werner, Stefan Mischke, Uwe Kissinger, Thomas Niendorf, Cornelia Wille, Stefanie Kaltenbach, Regina Giurato, Heiko Kohlmann, Dietmar Wendzel, Franca Kerz, Jana Pleitz, Antoine Leys, Nina Freitag, Irmgard Westenberger, Karin Siegmund, and Inge Burger of SCHOTT AG for their support with sample production, handling, measuring, and discussions. Christian Pahl from company Neutra for careful etching of tiles, Günter Kleer and Tobias Rist of the Fraunhofer Institute for Mechanics of Materials IWM in Freiburg, Germany, for their valuable measurements and especially Janina Krieg for her careful reading and many helpful suggestions for improvement of the manuscript and finally Thomas Westerhoff and Ralf Reiter for their continuing support.

References

1. T. Hull et al., "Use of updated material properties in parametric optimization of space borne mirrors," *Proc. SPIE* **9904**, 99046B (2016).
2. R. Jedamzik, T. Werner, and T. Westerhoff, "Production of the 4.26 m ZERODUR® mirror blank for the Advanced Technology Solar Telescope (ATST)," *Proc. SPIE* **9151**, 915131 (2014).
3. P. McNamara, S. Vitale, and K. Danzmann, "LISA Pathfinder," *Classical Quantum Gravity* **25**, 114034 (2008).
4. P. Hartmann et al., "ZERODUR® glass ceramics—strength data for the design of structures with high mechanical stresses," *Proc. SPIE* **7018**, 70180P (2008).
5. M. Cayrel et al., "ESO ELT Optomechanics: construction status," *Proc. SPIE* **10700**, 1070018 (2018).
6. S. W. Freiman, S. M. Wiederhorn, and J. J. Mecholsky Jr., "Environmentally enhanced fracture of glass: a historical perspective," *J. Am. Ceram. Soc.* **92**(7), 1371–1382 (2009).
7. W. Weibull, *A Statistical Theory of the Strength of Materials*, Ingeniörsvetenskapsakademiens Handlingar Nr 151. Generalstadens Litografiska Anstalts Förlag, Stockholm (1939).
8. W. Weibull, "A statistical distribution function of wide applicability," *ASME J. Appl. Mech.* **293** (1951).
9. T. Bizjak, P. Hartmann, and T. Westerhoff, "ZERODUR®—Bending strength data for tensile stress loaded support structures," *Proc. SPIE* **8326**, 83261Q (2012).
10. P. Hartmann, "ZERODUR®—Bending strength—review of achievements," *Proc. SPIE* **10371**, 1037104 (2017).
11. P. Hartmann, "ZERODUR®: deterministic approach for strength design," *Opt. Eng.* **51**(12), 124002 (2012).
12. A. A. Griffith, "The phenomena of rupture and flow in solids," *Phil. Trans. R. Soc. Lond. A* **221**, 163–198 (1921).
13. J. W. Peppi, "Strength properties of glass and ceramics," *SPIE Press Monograph* (2014) ISBN 0-81949-838-6.
14. S. M. Wiederhorn et al., "An error analysis of failure prediction techniques derived from fracture mechanics," *J. Am. Ceram. Soc.* **59**(9–10), 403–411 (1976).
15. ISO—International Standardization Organization, "ISO 6106: abrasive products—checking the grit size of super abrasives," International standard (2013).
16. CEN—European Committee for Standardization, "EN 1288-5 Determination of the bending strength of glass—Coaxial double ring

- test on flat specimens with small test surface areas,” European Standard (2000).
17. CEN—European Committee for Standardization, “EN 1288-1 Determination of the bending strength of glass—Fundamentals of testing glass,” European Standard (2000).
 18. R. Jedamzik, “ZERODUR®—Acid etching process in general,” *SCHOTT Process Description* (2007).
 19. I. J. Davies, “Unbiased estimation of Weibull modulus using linear least squares analysis—A systematic approach,” *J. Eur. Ceram. Soc.* **37**(1), 369–380 (2017).
 20. H. Rinne, *The Weibull Distribution*, CRC Press, Boca Raton, London, New York (2008).
 21. P. Hartmann, “ZERODUR® Strength modelling with Weibull statistical distributions,” *Proc. SPIE* **9912**, 991208 (2016).
 22. M. Ciccotti, “Stress-corrosion mechanisms in silicate glasses,” *J. Phys. D: Appl. Phys.* **42**, 214006 (2009).
 23. P. Hartmann, G. Kleer, and T. Rist, “ZERODUR®—New stress corrosion data improve strength fatigue prediction,” *Proc. SPIE* **9573**, 957304 (2015).
 24. T. A. Michalske, W. L. Smith, and E. P. Chen, “Stress intensity calibration for the double cleavage drilled compression specimen,” *Eng. Fract. Mech.* **45**(5), 637–642 (1993).
 25. P. Hartmann et al., “ZERODUR®—Bending strength data for etched surfaces,” *Proc. SPIE* **9151**, 91512Q (2014).
 26. P. Hartmann et al., “Double ring tests on ZERODUR® K20 and etched ZERODUR®,” in *Proc. 11th Eur. Conf. Spacecraft Struct. Mater. and Mech. Testing*, Toulouse, France (2009).
 27. Gemini Observatory, “Telescopes and Sites/Optics,” <https://www.gemini.edu/sciops/telescopes-and-sites/optics> (2016).
 28. P. Molloy et al., “Untersuchungen zur Oberflächenschädigung von ZERODUR®-Hohlzylindern durch Schleifrisse,” Report V 36/87 of the Fraunhofer-Institute IWM Freiburg (1987).
 29. X. Tonnellier et al., “Sub-surface damage issues for effective fabrication of large optics,” *Proc. SPIE* **7018**, 70180F (2008).
 30. A. Esmailzare, A. Rahimi, and S. M. Rezaei, “Investigation of subsurface damages and surface roughness in grinding process of ZERODUR® glass-ceramic,” *Appl. Surf. Sci.* **313**, 67–75 (2014).
 31. D. Tomka et al., “Development of methodology for evaluation of subsurface damage,” *Proc. SPIE* **9442**, 94421B (2015).
 32. G. Strothotte et al., “ZERODUR® micro crack depth reports 1991–2016,” *SCHOTT Internal Reports*.
 33. T. Lube and S. Béhar-LaFenêtre, “Strength behaviour of etched ZERODUR®,” *J. Eur. Ceram. Soc.* **37**, 4407–4413 (2017).
 34. R. Jedamzik et al., “The relation of surface treatment and sub-surface damage on ZERODUR®,” *Proc. SPIE* **10706**, 1070635 (2018).
 35. G. Exner, “Erlaubte Biegespannung in Glasbauteilen im Dauerlastfall,” *Glastech. Berichte* **56**(11), 299–312 (1983).
 36. A. G. Evans and S. M. Wiederhorn, “Proof testing of ceramic materials—an analytical basis for failure prediction,” *Int. J. Fract.* **26**, 355–368 (1984).
 37. F. Kerkhof, H. Richter, and D. Stahn, “Festigkeit von Glas Zur Abhängigkeit von Belastungsdauer und-verlauf,” *Glastech. Berichte* **54**(8), 265–277 (1981).
 38. T. Döhring et al., “Heritage of ZERODUR® glass ceramic for space applications,” *Proc. SPIE* **7425**, 74250L (2009).

Peter Hartmann received his doctorate degree in physics from the University of Mainz, Germany, in 1984. From 1985–2018, he has held different positions at advanced optics of SCHOTT AG Mainz. He served on the SPIE Board of Directors 2011–2013, on the Board of Trustees of the Max-Planck-Institute for Astronomy, Germany, and as convener of ISO and DIN working groups. He is a fellow of SPIE and a senior member of OSA.